A Fill Factor Loss Analysis Method for Silicon Wafer Solar Cells

Ankit Khanna, Thomas Mueller, Rolf A. Stangl, Bram Hoex, Prabir K. Basu, and Armin G. Aberle

***Abstract*—The fill factor of silicon wafer solar cells is strongly influenced by recombination currents and ohmic resistances. A practical upper limit for the fill factor of crystalline silicon solar cells operating under low-level injection is set by recombination in the quasi-neutral bulk and at the two cell surfaces. Series resistance, shunt resistance, and additional recombination currents further lower the fill factor. For process optimization or loss analysis of solar cells, it is important to determine the influence of both ohmic and recombination loss mechanisms on the fill factor. In this paper, a method is described to quantify the loss in fill factor due to series resistance, shunt resistance, and additional recombination currents. Only the 1-Sun *J–V* curve, series resistance at the maximum power point, and shunt resistance need to be determined to apply the method. Application of the method is demonstrated on an 18.4% efficient inline-diffused p-type silicon wafer solar cell and a 21.1% efficient heterojunction n-type silicon wafer solar cell. Our analysis does not require *J–V* curve fitting to extract diode saturation current densities or ideality factor; however, the results are shown to be consistent with curve fitting results if the cell's two-diode model parameters can be unambiguously determined by curve fitting.**

***Index Terms*—Crystalline silicon solar cells, fill factor, ohmic losses, recombination losses.**

I. Introduction

FOR silicon wafer solar cells, it is extremely important to achieve high fill factors to maximize the power generation capabilities of the cell. The fill factor of silicon wafer solar cells is strongly influenced by recombination currents and ohmic resistances. To account for these effects, the two-diode model of solar cells [1] is commonly used, which includes two diodes with saturation current densities J_{01}, J_{02}, and ohmic resistors $R_s, R_{\rm sh}$ in series and parallel to the diodes, respectively (see Fig. 1). The J_{01} diode describes recombination currents in the quasi-neutral bulk and the two cell surfaces. J_{02} recombination is most commonly attributed to SRH recombination [2], [3] in the space charge regions of the cell and an ideality factor $n_2 = 2$ is sometimes assigned to the J_{02} diode from SRH statistics [4], although deviations from this theoretical expectation have also been reported. Other proposed sources of J_{02} recombination are edge recombination [5] and recombination at localized regions with a high defect density [6], [7] which may lead to $n_2 > 2$. In this paper, we will refer to all recombination currents which do not follow the ideal-diode behavior as J_{02} recombination and treat n_2 as a variable cell parameter. Equation (1), shown below, represents the $J\ (V)$ equation for the two-diode model of solar cells

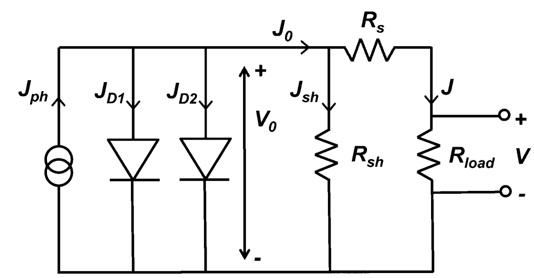

Fig. 1. Schematic of the two-diode model of a solar cell.

$$J = J_{\rm ph} - J_{01}[\exp\{q(V + JR_s)/kT\} - 1] - J_{02}[\exp\{q(V + JR_s)/n_2kT\} - 1] - (V + JR_s)/R_{\rm sh}. \quad (1)$$

We present a method to quantify the loss in fill factor for silicon wafer solar cells operating under low-level injection (LLI) due to series resistance, shunt resistance, and J_{02} recombination, based on the two-diode model. As a first step, a practical upper limit of fill factor is determined by assuming the absence of $R_s, R_{\rm sh}$, and J_{02}. Since the fill factor in this case depends on J_{01} recombination, we call it the "J_{01} limit" of fill factor. In subsequent steps, we quantify the losses in fill factor due to $R_s, R_{\rm sh}$, and J_{02}. Greulich *et al.* [8] and Hoenig *et al.* [9] have previously proposed using the difference between the J_{01} limit of fill factor and the pseudo fill factor, measured by the Suns-$V_{\rm oc}$ method [10], to quantify fill factor loss due to space charge region recombination. However, this approach is valid only if the effect of shunt resistance is negligible. In general, it is useful to consider the effects of a finite shunt resistance for an accurate loss analysis, especially for cells with high $V_{\rm oc}$. Our fill factor loss analysis does not involve fitting procedures to extract J_{01}, J_{02}, and n_2. The motivation for avoiding fitting procedures is to avoid assumptions about n_2. As mentioned earlier, the sources of J_{02} need not strictly follow an ideality factor of 2. In addition, the J_{02} recombination of a solar cell can arise from more than one source, and each J_{02} contributor may have a different ideality factor, which would again complicate fitting

Manuscript received January 21, 2013; revised April 30, 2013; accepted May 27, 2013. Date of publication July 9, 2013; date of current version September 18, 2013. The Solar Energy Research Institute of Singapore is sponsored by the National University of Singapore and Singapore's National Research Foundation (NRF) through the Singapore Economic Development Board. This work was supported by the NRF under Grant NRF2010EWT-CERP001-022.

The authors are with the Solar Energy Research Institute of Singapore, Singapore 117574 (e-mail: ankit.khanna@nus.edu.sg; thomas.mueller@nus.edu.sg; rolf.stangl@nus.edu.sg; bram.hoex@nus.edu.sg; prabir.basu@nus.edu.sg; armin.aberle@nus.edu.sg).

Color versions of one or more of the figures in this paper are available online at http://ieeexplore.ieee.org.

Digital Object Identifier 10.1109/JPHOTOV.2013.2270348

procedures. Hence, the method proposed here is independent of the ideality factor of the J_{02} current and directly quantifies the lumped effect of all J_{02} sources on fill factor. Only the 1-Sun *J–V* curve, series resistance at MPP, and shunt resistance need to be determined to apply the method. The method is discussed in the next section, followed by a rigorous analysis of the method's approximations. The method is demonstrated on an 18.4% efficient inline diffused p-type silicon wafer solar cell and a 21.1% efficient heterojunction n-type silicon wafer solar cell.

II. Fill Factor Loss Analysis Method

A. J_{01} *Limit of Fill Factor*

The J_{01} limit of fill factor (FF_{J01}) is determined by assuming the absence of R_s, $R_{\rm sh}$, and J_{02}. In this case, (1) reduces to

$$J = J_{\rm ph} - J_{01}\left[\exp(qV/kT) - 1\right]. \tag{2}$$

Imposing the conditions $J = 0$ at $V = V_{\rm oc}$ and $J = J_{\rm sc}$ at $V = 0$, (2) takes the form:

$$J = J_{\rm sc} - \frac{J_{\rm sc}}{\exp(qV_{\rm oc}/kT) - 1}\left[\exp(qV/kT) - 1\right]. \tag{3}$$

The fill factor of the *J–V* curve given by (3) is FF_{J01}. This procedure is used in this paper to determine FF_{J01}, but it is useful to also discuss analytical methods to determine FF_{J01}. FF_{J01} can be approximated analytically using the empirical formula proposed by Green [11]. Another method to obtain FF_{J01} is to use the Lambert W-Function [12] W, which provides an exact solution (derivation in the appendix) as stated in (4), although mathematical software is needed to evaluate the Lambert W-Function. For the cells analyzed in this paper, FF_{J01} determined by all three approaches discussed here matched within 0.01% absolute (for FF_{J01} in %)

$$FF_{J01} = \frac{kT}{qV_{\rm oc}}.\frac{(W[z]-1)^2\exp(W[z]-1)}{\exp(qV_{\rm oc}/kT) - 1}$$
$$z = \exp[1 + qV_{\rm oc}/kT]. \tag{4}$$

To apply the next steps of the fill factor loss analysis, we make an approximation that R_s, $R_{\rm sh}$, and J_{02} do not influence $J_{\rm sc}$ or $V_{\rm oc}$. For R_s and $R_{\rm sh}$, this approximation is valid within the range of these resistances determined in Section III-B (for the validity of a separate approximation introduced in the next step); therefore, the influence of R_s and $R_{\rm sh}$ on $J_{\rm sc}$ and $V_{\rm oc}$ is not separately discussed. While J_{02} affects both $V_{\rm oc}$ and *FF*, at high voltages the J_{01} current dominates the cell's electrical characteristics and the effect of J_{02} on $V_{\rm oc}$ is small. We will revisit this approximation in Section III-A.

B. *Fill Factor Loss due to* R_s *and* $R_{\rm sh}$

Considering the two-diode model at MPP (see Fig. 1), the terminal voltage and current density (subscript mpp added to V and J) will be related to R_s and $R_{\rm sh}$ by

$$V_{\rm mpp} = V_0 - J_{\rm mpp}R_s \tag{5}$$

$$J_{\rm mpp} = J_0 - (V_{\rm mpp} + J_{\rm mpp}R_s)/R_{\rm sh}. \tag{6}$$

From (5) and (6), the product V_0J_0 can be determined and normalized with $V_{\rm oc}J_{\rm sc}$ to obtain

$$\frac{V_0J_0}{V_{\rm oc}J_{\rm sc}} = \frac{V_{\rm mpp}J_{\rm mpp}}{V_{\rm oc}J_{\rm sc}} + \frac{J_{\rm mpp}^2R_s}{V_{\rm oc}J_{\rm sc}} + \frac{(V_{\rm mpp} + J_{\rm mpp}R_s)^2}{R_{\rm sh}V_{\rm oc}J_{\rm sc}}. \tag{7}$$

We make an approximation here that V_0, J_0 is the MPP of the resistance-free cell. This is equivalent to the approximation that R_s only shifts $V_{\rm mpp}$ and $R_{\rm sh}$ only shifts $J_{\rm mpp}$. In general, V_0, J_0 will not be the MPP of the resistance-free solar cell; however, it will be sufficiently close to the MPP for a range of R_s and $R_{\rm sh}$. The error due to this approximation is discussed in Section III-B. Under this approximation, the fill factor of the resistance-free cell FF_0 will be related to the fill factor of the real cell *FF* by

$$FF_0 = FF + \frac{J_{\rm mpp}^2R_s}{V_{\rm oc}J_{\rm sc}} + \frac{(V_{\rm mpp} + J_{\rm mpp}R_s)^2}{R_{\rm sh}V_{\rm oc}J_{\rm sc}}. \tag{8}$$

The second and third terms on the right-hand side of (8) are the fill factor losses due to R_s and $R_{\rm sh}$: $\Delta FF_{\rm Rs}$ and $\Delta FF_{R\rm sh}$. Since we obtain these terms at MPP using measured R_s at MPP, no error is expected due to distributed resistance effects [13]

$$\Delta FF_{Rs} = J_{\rm mpp}^2R_s/V_{\rm oc}J_{\rm sc} \tag{9}$$

$$\Delta FF_{R\rm sh} = (V_{\rm mpp} + J_{\rm mpp}R_s)^2/R_{\rm sh}V_{\rm oc}J_{\rm sc}. \tag{10}$$

C. *Fill Factor Loss due to* J_{02} *Recombination*

The loss in fill factor due to J_{02} recombination, ΔFF_{J02}, is the difference between the J_{01} limit of fill factor, FF_{J01}, and the resistance free fill factor, FF_0. Thus, (9)–(11) specify the fill factor loss due to R_s, $R_{\rm sh}$, and J_{02} recombination

$$\Delta FF_{J02} = FF_{J01} - FF_0. \tag{11}$$

III. Error Analysis

We will now analyze the approximations made in the previous section individually to obtain a range of R_s, $R_{\rm sh}$, and J_{02} for which the error is within acceptable limits.

A. *Approximation:* J_{02} *Recombination Does Not Influence* $V_{\rm oc}$

If the effect of J_{02} on $V_{\rm oc}$ is neglected, and the measured $V_{\rm oc}$ (which includes the influence of J_{02}) is used to determine FF_{J01}, then FF_{J01} will be underestimated. Since the resistance corrected fill factor FF_0 includes the effect of J_{02} recombination, this approximation does not introduce an error in FF_0. Thus, from (11), ΔFF_{J02} will also be underestimated. To analyze this error, we define two sets of baseline (one-diode ideal) simulation parameters summarized in Table I. Baseline 1 represents a typical diffused-emitter p-type silicon wafer solar cell, and Baseline 2 represents a high-efficiency n-type silicon wafer solar cell. For Baseline 2, $V_{\rm oc}$ and $J_{\rm sc}$ reported in [14] are used as an approximate reference.

The drop in $V_{\rm oc}$ when a J_{02} term (taking $n_2 = 2$) is introduced to the baseline models is shown in Fig. 2 (top). It is clear that cells with higher $V_{\rm oc}$ will be affected more strongly by the presence of J_{02} recombination. The relative error in ΔFF_{J02}

TABLE I
BASELINE PARAMETERS USED TO DETERMINE THE ERROR IN FF_{J01}

Description	Cell parameter	Baseline 1 (standard cell)	Baseline 2 (high-eff. cell)
Simulation input parameter	J_{01} (A/cm^2)	1x10^{-12}	2.5x10^{-14}
	J_{ph} (mA/cm^2)	37.0	40.5
Resulting cell parameter	V_{oc} (mV) for J_{02} =0	625.3	722.4
	FF_{J01} (%)	83.3	85.0

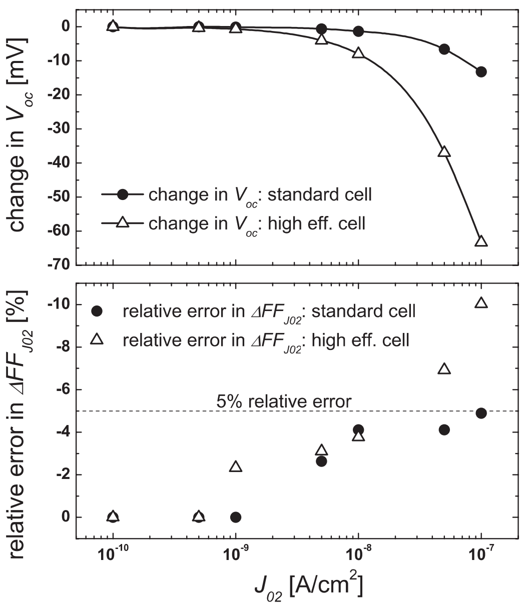

Fig. 2. (Top) Change in $V_{\rm oc}$ as a function of J_{02} according to a two-diode simulation for the baseline parameters in Table I. (Bottom) Relative error in ΔFF_{J02} as a function of J_{02}. Top and bottom graphs have the same x-axis.

is shown in Fig. 2 (bottom). The negative sign indicates that ΔFF_{J02} is underestimated. It can be seen that for the standard cell, ΔFF_{J02} is within a relative error limit of 5% for J_{02} values up to 10^{-7}A/cm^2. For the high-efficiency cell, however, the relative error reaches 10% when J_{02} reaches 10^{-7}A/cm^2.

B. Approximation: R_s Only Shifts $V_{\rm mpp}$ and $R_{\rm sh}$ Only Shifts $J_{\rm mpp}$

The fill factor losses due to R_s and $R_{\rm sh}$ are calculated under this approximation. However, from the two-diode model, it can be seen that the presence of either R_s or $R_{\rm sh}$ shifts the MPP in terms of both current density and voltage (see Fig. 3).

We analyzed the error due to this approximation by comparing the fill factor losses due to R_s and $R_{\rm sh}$ calculated by (9) and (10) with the exact fill factor loss determined by the two-diode simulation. As in the previous section, we used the two sets of baseline parameters (see Table I) with an additional J_{02} term ($J_{02} = 1.0 \times 10^{-9}A/cm^2, n_2 = 2$) added to both baselines. The relative errors in ΔFF_{Rs} and $\Delta FF_{R\rm sh}$ are shown in Fig. 4.

For both the standard cell and the high-efficiency cell, the relative errors in ΔFF_{Rs} and $\Delta FF_{R\rm sh}$ are within the 5% limit for $R_s < 4\,\Omega\cdot$cm^2 and $R_{\rm sh} > 50\,\Omega\cdot$cm^2. The negative sign indicates that ΔFF_{Rs} and $\Delta FF_{R\rm sh}$ are underestimated. However, the error criteria for ΔFF_{Rs} and $\Delta FF_{R\rm sh}$ need to be more stringent

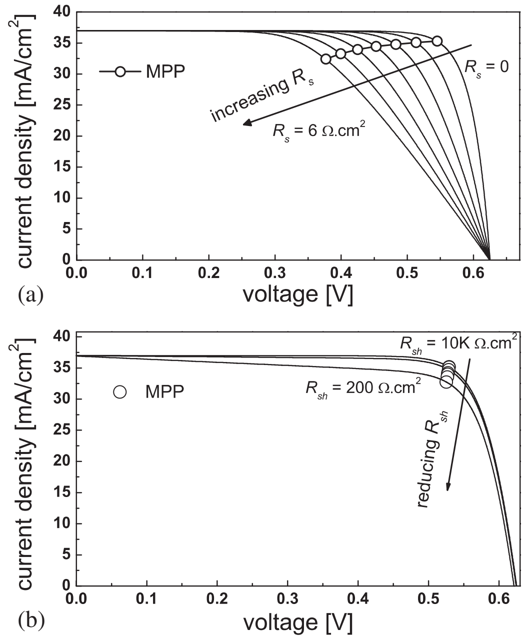

Fig. 3. Effect of (a) increasing R_s and (b) reducing $R_{\rm sh}$ on the *J–V* curve of solar cells. The curves were obtained by a two-diode simulation with baseline parameters $J_{01} = 10^{-12}$A/cm$^2, J_{02} = 10^{-9}$A/cm$^2, n_2 = 2$, $J_{\rm ph} =$ 37 mA/cm$^2, R_{\rm sh} = 10$ k$\Omega\cdot$cm^2 for (a) and $R_s = 0.5\ \Omega\cdot$cm^2 for (b). For clarity, some intermediate *J–V* curves have been omitted from (b), and only the MPPs are shown.

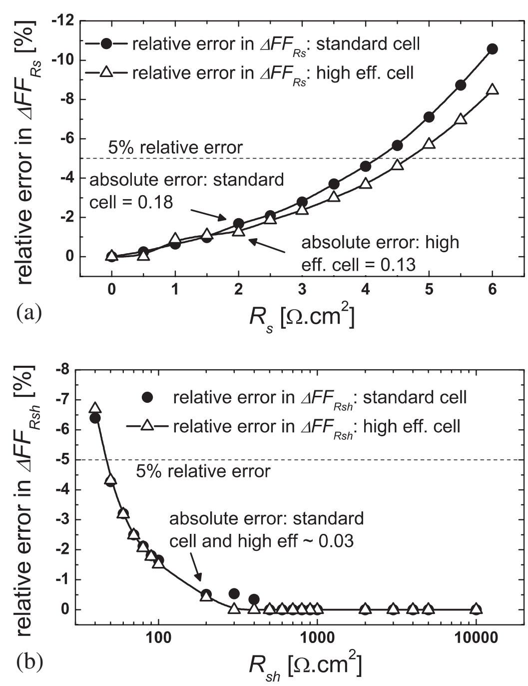

Fig. 4. Relative error in (a) ΔFF_{Rs} as a function of R_s and (b) $\Delta FF_{R\rm sh}$ as a function of $R_{\rm sh}$.

because the error in these terms is transferred to ΔFF_{J02} according to (8) and (11). If the absolute errors in ΔFF_{Rs} and $\Delta FF_{R\rm sh}$ are $\delta(\Delta FF_{Rs})$ and $\delta(\Delta FF_{R\rm sh})$, respectively, then the absolute error in $\Delta FF_{J02}, \delta(\Delta FF_{J02})$ will be given by

$$\delta(\Delta FF_{J02}) = -\delta(\Delta FF_{Rs}) - \delta(\Delta FF_{R\rm sh}). \qquad (12)$$

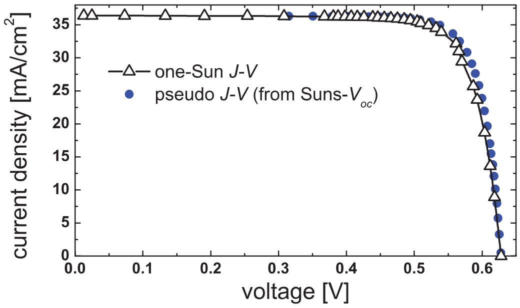

Fig. 5. 1-Sun *J–V* curve and Suns-$V_{\rm oc}$ curve of the inline-diffused cell.

Hence, we would like to ensure that the sum of the absolute errors in ΔFF_{Rs} and $\Delta FF_{R\rm sh}$ is limited to ~0.2 (for all fill factor terms in %). This would be the case for $R_s < 2\ \Omega{\cdot}{\rm cm}^2$ and $R_{\rm sh} > 200\ \Omega{\cdot}{\rm cm}^2$ for both the standard and the high-efficiency cell.

As a rule of thumb, the errors due to the approximations made in our fill factor loss analysis method will be small when $R_s < 2\ \Omega{\cdot}{\rm cm}^2, R_{\rm sh} > 200\ \Omega{\cdot}{\rm cm}^2$, and $J_{02} < 10^{-7}{\rm A/cm}^2$. This is likely to cover the entire practically important range of these quantities for silicon wafer solar cells.

IV. Examples of Application of the Method

In this section, we demonstrate the application of the fill factor loss analysis method to an inline-diffused p-type silicon wafer solar cell and a heterojunction n-type silicon wafer solar cell.

A. Inline-Diffused p-Type Silicon Wafer Cell

The inline-diffused cell investigated here has a 1.6 Ω·cm p-type Cz wafer base (area 239 cm^2) and an n$^+$ inline-diffused homogeneous emitter. Front and rear contacts were formed by screen printing and cofiring of a front silver grid (H pattern) and rear full-area aluminum contact. A detailed description of the inline diffusion process is given in [15]. The 1-Sun *J–V* and the pseudo *J–V* (from Suns-$V_{\rm oc}$) curves of the cell measured on a 1-Sun flash tester (Sinton Instruments) are shown in Fig. 5, and the *J–V* parameters are summarized in Table II. R_s at MPP was determined from the voltage shift at $J_{\rm mpp}$ between the 1-Sun *J–V* curve and the Suns-$V_{\rm oc}$ curve [10]. $R_{\rm sh}$ was determined by the inverse of the slope of a linear fit to the cell's dark *J–V* curve (not shown here) in the range 0–50 mV. *pFF* represents the pseudo fill factor obtained from the Suns-$V_{\rm oc}$ curve (82.6%) which as expected closely matches the sum of the measured fill factor and the ΔFF_{Rs} term (82.5%). Measurement of the Suns-$V_{\rm oc}$ curve or the *pFF* is not necessary to apply the fill factor loss analysis since R_s at MPP may be obtained by other methods, e.g., 1) comparison of the 1-Sun *J–V* curve and the shifted dark *J–V* curve [13] and 2) comparison of two or more *J–V* curves at different illumination intensities [1], [16].

The fill factor loss analysis of this solar cell reveals that FF_{J01} is 83.4%, and the drop to the cell's measured fill factor of 80.4% is primarily caused by series resistance (see Table II). The sources of series resistance of this cell were analyzed individually based on the unit cell approach of Mette [17]. The parameters used for determining the series resistance components and the calculated series resistance components are summarized in Tables III and IV, respectively. All resistance components are within the limits expected from a screen-printed silicon wafer solar cell. The close match between the calculated sum of series resistance components and the measured R_s at MPP indicates optimized processing. Hence, without altering the present process flow, only a small improvement in fill factor can be expected via a lowering of the series resistance. A more effective route to improve the cell's fill factor is, therefore, to improve the shunt resistance and address the sources of J_{02} recombination. The shunt resistance can be improved by an optimization of the chemical edge isolation step used for this cell. To reduce J_{02} recombination, the inline diffusion step or the contact firing step may need further optimization.

We had earlier indicated our motivation to avoid fitting procedures to extract J_{01}, J_{02}, and ideality factor. However, the Suns-$V_{\rm oc}$ curve for the inline-diffused cell fits the two-diode model very well [see Fig. 6(a)], and it is possible to unambiguously determine parameters of the two-diode model ($R_{\rm sh}$ was fixed to the value determined earlier and J_{01}, J_{02}, and n_2 were fitted here). Hence, the fill factor loss terms for at least this cell can also be determined by simulation of the two-diode model based on measured and fitted parameters. This was done by simulating the *J–V* curve with J_{01} alone and sequentially including J_{02}, R_s (measured R_s at MPP), and $R_{\rm sh}$ to the *J–V* curve [see Fig. 6(b)]. The results obtained [see Fig. 6(b)] agree exactly with the fill factor loss analysis results (see Table II). We also compared our fill factor loss analysis results (see Table II) with the Greulich/Hoenig approach [8], [9] (i.e., $\Delta FF_{R\rm sh}$ is assumed to be 0, $\Delta FF_{Rs} = pFF - FF$, $\Delta FF_{J02} = FF_{J01} - pFF$) which leads to $FF_{J01} = 83.4\%$, $\Delta FF_{Rs} = 2.2\%$, $\Delta FF_{R\rm sh} = 0$, and $\Delta FF_{J02} = 0.8\%$. The Greulich/Hoenig approach in this case overapproximates ΔFF_{J02} by 0.2% absolute by ignoring the losses across $R_{\rm sh}$ and, hence, additionally attributing the fill factor loss across $R_{\rm sh}$ to J_{02}. This illustrates that the influence of $R_{\rm sh}$ should be considered for an accurate fill factor loss analysis. It is relevant to mention here that both our fill factor loss analysis and the Greulich/Hoeing approach are influenced in the same way by the approximation discussed in Section III-A. For the approximation discussed in Section III-B, the error (our analysis) in the inline-diffused cell's ΔFF_{J02} term due to the R_s and $R_{\rm sh}$ (0.41 Ω·cm^2 and 4.3 kΩ·cm^2) is $< 0.01\%$ absolute.

B. Heterojunction n-Type Silicon Wafer Solar Cell

The heterojunction silicon wafer solar cell that is investigated here (see Fig. 7) has a 1 Ω·cm n-type FZ wafer base (active device area 1.0 cm^2) with intrinsic amorphous silicon suboxides (a-SiO$_x$:H) as interface passivation layers. A detailed discussion for this cell structure is given in [18]. The 1-Sun *J–V* curve for the cell measured on a 1-Sun *J–V* tester (steady-state light source, WACOM) and the Suns-$V_{\rm oc}$ curve measured on a Sinton Suns-$V_{\rm oc}$ tester are shown in Fig. 8, and the *J–V* parameters are summarized in Table V. R_s at MPP and $R_{\rm sh}$ were determined using the same procedures mentioned earlier for the inline-diffused cell. The R_s value reported in [18] was determined

TABLE II
1-Sun *J–V* Data and Fill Factor Loss Analysis Results for the Inline-Diffused Cell

Cell parameters										FF loss analysis results			
Area (cm^2)	V_{oc} (mV)	J_{sc} (mA/cm^2)	FF (%)	Eff. (%)	V_{mpp} (mV)	J_{mpp} (mA/cm^2)	R_s at MPP (Ωcm^2)	R_{sh} (Ωcm^2)	pFF (%)	FF_{J01} (%)	ΔFF_{Rs} (% absolute)	ΔFF_{Rsh}	ΔFF_{J02}
239	627.9	36.4	80.4	18.4	532.2	34.5	0.41	4.3x10^3	82.6	83.4	2.1	0.3	0.6

TABLE III
Parameters Used to Calculate Series Resistance Components

S. No	Parameter	Value
1	Front electrode design	79 fingers, 3 busbars
2	Wafer thickness (after texturing)	~ 170 µm
3	Finger width	90 µm
4	Busbar width	1.5 mm
5	Emitter sheet resistance	70 Ω/□
6	Specific contact resistance	1 mΩcm^2
7	Front metal paste sheet resistance	1.8 mΩ/□

TABLE IV
Calculated Series Resistance Components

Component	Front busbar	Front fingers	Front contact	Emitter	Base	Total
Resistance (Ωcm^2)	0.02	0.09	0.03	0.22	0.03	0.39

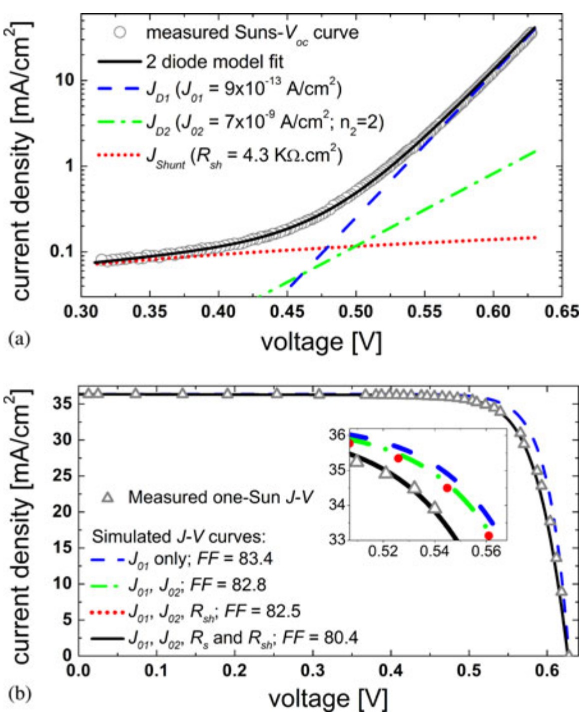

Fig. 6. (a) Two-diode model fit to the measured Suns-$V_{\rm oc}$ curve of the inline-diffused cell. (b) Simulated *J–V* curves using measured and fitted parameters. For clarity, two intermediate *J–V* curves are shown only in the inset.

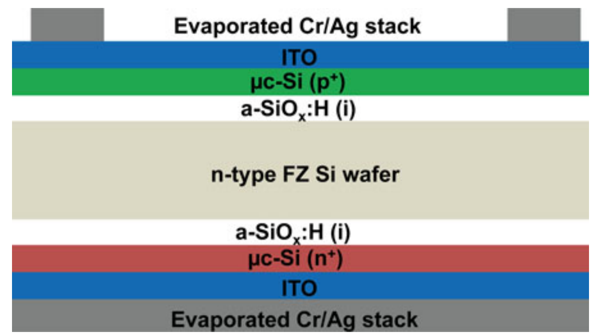

Fig. 7. Schematic of the heterojunction cell (texture omitted for clarity).

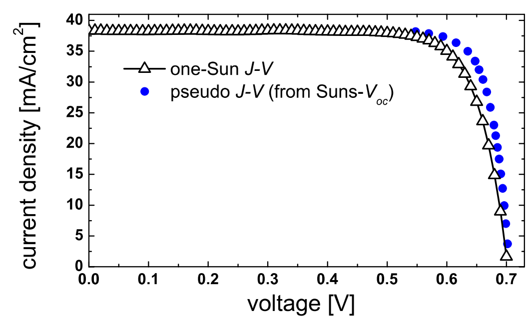

Fig. 8. 1-Sun *J–V* curve and Suns-$V_{\rm oc}$ curve of the heterojunction cell.

from the slope of the 1-Sun *J–V* curve at 800 mV; however, this is not an appropriate parameter for fill factor loss analysis and is not used here.

Due to the high $V_{\rm oc}$ of the heterojunction cell, it is important to check if the cell operates under LLI for most of the range between $V_{\rm mpp}$ and $V_{\rm oc}$. An approximate check for LLI is to convert the quasi-Fermi level splitting under open-circuit conditions to injected carrier density (Δn) and to compare this with the wafer doping (N_d for an n-type wafer). This leads to (13) if the cell is under LLI even under open-circuit conditions [19]. n_i is the intrinsic carrier concentration for Si

$$V_{\rm oc} < 2(kT/q)\ln[N_d/n_i]. \tag{13}$$

The 1 Ω·cm resistivity of the heterojunction cell corresponds to a doping of 5 × 10^{15} cm^{-3}, and the term on the right side of (13) is 682 mV. Since $V_{\rm oc}$ of the heterojunction cell is 20 mV higher than this limit, the cell's bulk is likely to operate under the onset of high-level injection (HLI) conditions near open circuit. However, for most of the range between $V_{\rm mpp}$ (590 mV) and $V_{\rm oc}$ (702 mV), the bulk lies in LLI, and hence, the influence of this transition on fill factor is probably small and is not considered here. Application of the fill factor loss analysis indicates that FF_{J01} is 84.7%, and significant losses in fill factor are caused by R_s and J_{02} leading to a measured fill factor of 78.6%. $R_{\rm sh}$ for this heterojunction cell is very high, and no losses occur across it. Again, the sum of the measured fill factor and the ΔFF_{Rs} term (83.4%) closely matches the *pFF* obtained from the Suns-$V_{\rm oc}$ curve (83.3%). Furthermore, the Suns-$V_{\rm oc}$ curve of the heterojunction also gave a reasonable fit to the two-diode model [see Fig. 9(a)], and we repeated the fitting and simulation procedure, as discussed earlier. The results obtained [see Fig. 9(b)] were

TABLE V
1-SUN *J–V* DATA AND FILL FACTOR LOSS ANALYSIS RESULTS FOR THE HETEROJUNCTION CELL

Cell parameters										FF loss analysis results			
Area (cm^2)	V_{oc} (mV)	J_{sc} (mA/cm^2)	FF (%)	Eff. (%)	V_{mpp} (mV)	J_{mpp} (mA/cm^2)	R_s at MPP (Ωcm^2)	R_{sh} (Ωcm^2)	pFF (%)	FF_{J01} (%)	ΔFF_{Rs} (% absolute)	ΔFF_{Rsh}	ΔFF_{J02}
1.0	702.2	38.3	78.6	21.1	590	35.8	1.0	$1x10^6$	83.3	84.7	4.8	0.0	1.3

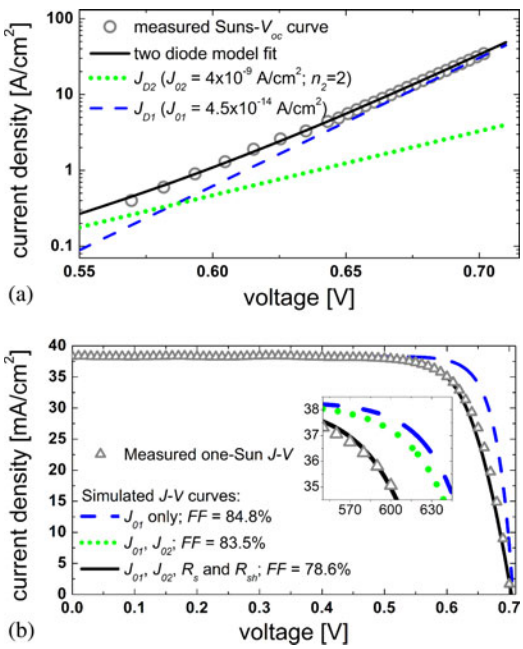

Fig. 9. (a) Two-diode model fit to the measured Suns-$V_{\rm oc}$ curve of the heterojunction cell. (b) Simulated *J–V* curves using measured and fitted parameters. For clarity, an intermediate *J–V* curve is shown only in the inset.

in good agreement (all terms match within 0.1% absolute) with the fill factor loss analysis (see Table V). We again compared our results for the heterojunction cell with the Greulich/Hoeing approach [8], [9], leading to $FF_{J01} = 84.7\%$, $\Delta FF_{Rs} = 4.7\%$, $\Delta FF_{R\rm sh} = 0$, and $\Delta FF_{J02} = 1.4\%$. In this case, as $\Delta FF_{R\rm sh}$ is indeed zero, there is good agreement between these two approaches (all terms match within 0.1% absolute).

V. DISCUSSION OF INJECTION-DEPENDENT EFFECTS

The fill factor loss analysis method presented in this paper is based on the two-diode model of solar cells, where we assume that J_{01} is not injection dependent and follows an ideality factor of 1. No assumptions are made about the ideality factor of the J_{02} term, and it may vary based on the source of J_{02} recombination. The conditions regarding J_{01} are valid under LLI in the absence of strong injection-dependent effects in the bulk and on the cell's two surfaces. The LLI condition can be verified for a cell by (13). If the bulk undergoes a transition from LLI to the onset of HLI close to $V_{\rm oc}$ (as was the case for the heterojunction cell discussed earlier), then this transition is only likely to have a small influence on fill factor. However, if the transition occurs close to $V_{\rm mpp}$, then the fill factor will be additionally strongly affected by the onset of HLI. Other known injection-dependent effects that can influence fill factors (even when the LLI condition is fulfilled) are injection-dependent bulk lifetimes in boron doped Cz or multicrystalline wafers due boron-oxygen-related defects [20] and injection-dependent surface recombination at SiO_2 passivated Si rear surfaces [21]. For cells affected by such injection-dependent effects, the ΔFF_{J02} term calculated by our method will additionally include the influence of injection-dependent effects on fill factor, since this term is obtained directly by the difference between FF_{J01} and the resistance corrected FF_0. In such cases, the gap between FF_{J01} and the measured *FF* will be attributed to R_s, $R_{\rm sh}$, and the lumped effect of J_{02} recombination and injection-dependent effects on fill factor. Within the framework of this simple analysis, it is not possible to separate the influence of J_{02} recombination and injection-dependent effects on fill factor.

VI. CONCLUSION

A method was described to analyze the fill factor losses of silicon wafer solar cells due to series resistance, shunt resistance, and J_{02} recombination. An error analysis revealed that the error due the method's simplifying approximations is sufficiently small when $R_s < 2\ \Omega{\cdot}\rm cm^2$, $R_{\rm sh} > 200\ \Omega{\cdot}\rm cm^2$, and $J_{02} < 10^{-7}\,\rm A/cm^2$. This range is likely to cover the entire practically important range of these quantities for silicon wafer solar cells. Application of the fill factor loss analysis was demonstrated on an 18.4% efficient inline-diffused p-type silicon wafer solar cell and 21.1% efficient heterojunction n-type silicon wafer solar cell. It was further shown that if the two-diode model parameters can be unambiguously determined from a fitting of the cell's Suns-$V_{\rm oc}$ curve, then the fill factor losses determined by simulation of the cell's diode models with measured and fitted parameters closely match the results of the fill factor loss analysis method presented here. Limitations of the method for solar cells strongly affected by injection-dependent effects were also discussed.

APPENDIX

The Lambert W-Function [12] W is defined as the inverse function of the function $f(x) = x\ \exp(x)$. While there is no simple expression for W, it can be easily evaluated using mathematical software like Mathematica. The Lambert W-Function is useful to solve transcendental equations involving exponential terms and has been previously used for solar cell analysis to extract cell parameters from measured *I–V* curves [22], [23]. Here, we will use this function to obtain an exact expression for FF_{J01}. We first define $V_{\rm mpp0}$, $J_{\rm mpp0}$ as the MPP for the hypothetical case when the absence of R_s, $R_{\rm sh}$, and J_{02} is assumed, i.e., the J_{01} limit described in Section II-A. In addition, from the definition of W, we note the following property, which will be subsequently used:

$$W[x\exp(x)] = x. \tag{A1}$$

We start with the maximum power condition, i.e., $d(JV)/dV = 0$ at $V = V_{\mathrm{mpp0}}$, and substitute J from (3). This leads to

$$J_{\mathrm{sc}} \frac{d}{dV}\left[V - \frac{V\{\exp(qV/kT)-1\}}{\exp(qV_{\mathrm{oc}}/kT)-1}\right] = 0 \text{ at } V = V_{\mathrm{mpp0}}. \tag{A2}$$

Differentiating and setting $V = V_{\mathrm{mpp0}}$ yields

$$\exp(qV_{\mathrm{oc}}/kT) = (1 + qV_{\mathrm{mpp0}}/kT)\exp(qV_{\mathrm{mpp0}}/kT). \tag{A3}$$

Multiplying both sides by exp(1), we get

$$\exp(1 + qV_{\mathrm{oc}}/kT) = (1 + qV_{\mathrm{mpp0}}/kT)\exp(1 + qV_{\mathrm{mpp0}}/kT). \tag{A4}$$

We now use the terms on both sides of (A4) as arguments for the Lambert W-Function and use the property stated in (A1). This leads to

$$W[\exp(1 + qV_{\mathrm{oc}}/kT)] = (1 + qV_{\mathrm{mpp0}}/kT). \tag{A5}$$

FF_{J01} can now be computed as

$$FF_{J01} = (V_{\mathrm{mpp0}} J_{\mathrm{mpp0}})/V_{\mathrm{oc}} J_{\mathrm{sc}}. \tag{A6}$$

J_{mpp0} is substituted from (3) with $V = V_{\mathrm{mpp0}}$, and some simplification leads to

$$FF_{J01} = \left(\frac{V_{\mathrm{mpp0}}}{V_{\mathrm{oc}}}\right)\left[\frac{\exp(qV_{\mathrm{oc}}/kT) - \exp(qV_{\mathrm{mpp0}}/kT)}{\exp(qV_{\mathrm{oc}}/kT) - 1}\right]. \tag{A7}$$

Substituting for $\exp(qV_{\mathrm{oc}}/kT)$ from (A3) yields

$$FF_{J01} = \left(\frac{qV_{\mathrm{mpp0}}^2}{kTV_{\mathrm{oc}}}\right)\left[\frac{\exp(qV_{\mathrm{mpp0}}/kT)}{\exp(qV_{\mathrm{oc}}/kT) - 1}\right]. \tag{A8}$$

Substituting for V_{mpp0} from (A5) leads to the expression for FF_{J01} using the Lambert W-Function, as previously stated in (4):

$$FF_{J01} = \frac{kT}{qV_{\mathrm{oc}}} . \frac{(W[z]-1)^2 \exp(W[z]-1)}{\exp(qV_{\mathrm{oc}}/kT) - 1}$$
$$z = \exp[1 + qV_{\mathrm{oc}}/kT]. \tag{A9}$$

REFERENCES

[1] M. Wolf and H. Rauschenbach, "Series resistance effects on solar cell measurements," *Adv. Energy Convers.*, vol. 3, pp. 455–479, 1963.

[2] W. Shockley and W. T. Read, "Statistics of the recombination of holes and electrons," *Phys. Rev.*, vol. 87, pp. 835–842, 1952.

[3] R. N. Hall, "Electron-hole recombination in germanium," *Phys. Rev.*, vol. 87, pp. 387–387, 1952.

[4] C. T. Sah, R. Noyce, and W. Shockley, "Carrier generation and recombination in p-n Junctions and p-n junction characteristics," *Proc. IRE*, vol. 45, pp. 228–1243, 1957.

[5] K. McIntosh, "Lumps, humps and bumps: Three detrimental effects in the current-voltage curve of silicon solar cells," Ph.D. dissertation, Centre Photovolt. Eng., Univ. New South Wales, Sydney, Australia, 2001.

[6] O. Breitenstein, J. P. Rakotoniaina, and M. H. Al Rifai, "Shunt types in crystalline silicon solar cells," *Prog. Photovolt.*, vol. 12, pp. 529–538, 2004.

[7] S. Steingrube, O. Breitenstein, K. Ramspeck, S. Glunz, A. Schenk, and P. P. Altermatt, "Explanation of commonly observed shunt currents in c-Si solar cells by means of recombination statistics beyond the Shockley-Read-Hall approximation," *J. Appl. Phys.*, vol. 110, 014515, pp. 1–10, 2011.

[8] J. Greulich, M. Glatthlaar, and S. Rein, "Fill factor analysis of solar cells' current-voltage curves," *Prog. Photovolt.*, vol. 18, pp. 511–515, 2010.

[9] R. Hoenig, M. Glatthaar, F. Clement, J. Greulich, J. Wilde, and D. Biro, "New measurement method for the investigation of space charge region recombination losses induced by the metallization of silicon solar cells," *Energy Procedia*, vol. 8, pp. 694–699, 2011.

[10] R. Sinton and A. Cuevas, "A quasi-steady-state open-circuit voltage method for solar cell characterization," in *Proc. 16th Eur. Photovolt. Solar Energy Conf.*, Glasgow, U.K., 2000, pp. 1152–1155.

[11] M. A. Green, "Accuracy of analytical expressions for solar cell fill factors," *Solar Cells*, vol. 7, pp. 337–340, 1982.

[12] E. W. Weisstein. (2013, Jan.). Lambert W-Function, from Wolfram MathWorld [Online]. Available: http://mathworld.wolfram.com/LambertW-Function.html

[13] A. G. Aberle, S. R. Wenham, and M. A. Green, "A new method for accurate measurements of the lumped series resistance of solar cells," in *Proc. 23rd IEEE Photovolt. Spec. Conf.*, Louisville, KY, USA, 1993, pp. 133–138.

[14] P. Cousins, D. Smith, H. Luan, J. Manning, T. Dennis, A. Waldhauer, K. Wilson, G. Harley, and W. Mulligan, "Generation 3: Improved performance at lower cost," in *Proc. 35th IEEE Photovolt. Spec. Conf.*, 2010, HI, USA, pp. 275–278.

[15] P. K. Basu, M. B. Boreland, K. D. Shetty, D. Sarangi, and A. G. Aberle, "18.3% efficient inline diffused emitter silicon wafer solar cells," in *Proc. Tech. Dig. Photovolt. Solar Energy Conf. Exhib.*, Fukuoka, Japan, 2011.

[16] K. C. Fong, K. R. McIntosh, and A. W. Blakers, "Accurate series resistance measurement of solar cells," *Prog. Photovolt.: Res. Appl.*, vol. 21, pp. 490–499, 2013.

[17] A. Mette, "New concepts for front side metallization of industrial silicon solar cells," Ph.D. dissertation, Dep. Appl. Sci., Univ. Freiburg, Freiburg, Germany, pp. 16–17, 2007.

[18] T. Mueller, J. Wong, and A. G. Aberle, "Heterojunction silicon wafer solar cells using amorphous silicon suboxides for interface passivation," *Energy Procedia*, vol. 15, pp. 97–106, 2012.

[19] P. J. Verlinden, M. Aleman, N. Posthuma, J. Fernandez, B. Pawlak, J. Robbelein, M. Debucquoy, K.V. Wichelen, and J. Poortmans, "Simple power-loss analysis method for high-efficiency interdigitated back contact (IBC) silicon solar cells," *Solar Energy Mater. Solar Cells*, vol. 106, pp. 37–41, 2012.

[20] K. Bothe, R. Sinton, and J. Schmidt, "Fundamental boron-oxygen-related carrier lifetime limit in mono- and multicrystalline silicon," *Prog. Photovolt.*, vol. 13, pp. 287–296, 2005.

[21] A. G. Aberle, S. J. Robinson, A. Wang, J. Zhao, S.R. Wenham, and M. A. Green, "High-efficiency silicon solar cells: Fill factor limitations and non-ideal diode behaviour due to voltage-dependent rear surface recombination velocity," *Prog. Photovolt.*, vol. 1, pp. 133–143, 1993.

[22] A. Jain and A. Kapoor, "Exact analytical solutions of the parameters of real solar cells using Lambert W-function," *Solar Energy Mater. Solar Cells*, vol. 81, pp. 269–277, 2003.

[23] A. Jain and A. Kapoor, "A new method to determine the diode ideality factor of real solar cell using Lambert W-function," *Solar Energy Mater. Solar Cells*, vol. 85, pp. 391–396, 2005.

Ankit Khanna received the Master of Technology degree in engineering physics from the Indian Institute of Technology (Banaras Hindu University), Varanasi, India, in 2010. Since 2011, he has been working toward the Ph.D. degree with the Solar Energy Research Institute of Singapore, Singapore, focusing on metallization methods for silicon wafer solar cells.

Thomas Mueller received the Diploma degree in electrical engineering from the University of Dortmund, Dortmund, Germany, and the Ph.D. degree from the University of Hagen, Hagen, Germany.

He is the Head with the Silicon Wafer Solar Cells I Group of the Solar Energy Research Institute of Singapore, Singapore. His research focuses on advanced high-efficiency silicon wafer solar cell architectures such as all-back-contact and heterojunction cells.

Rolf A. Stangl received the Ph.D. degree in organic solar cells for work conducted with the Fraunhofer Institute for Solar Energy Systems, Freiburg, Germany.

He is a Senior Research Scientist with the Solar Energy Research Institute of Singapore, Singapore. He is a Project Leader for hybrid heterojunction solar cells and a competence Team Leader for electrical characterization/simulation.

Bram Hoex received the M.Sc. and Ph.D. degrees in applied physics from the Eindhoven University of Technology, Eindhoven, The Netherlands.

He is a Director and Group Leader with the Silicon Materials and Cells Cluster, Solar Energy Research Institute of Singapore, Singapore. His research focuses on advanced fabrication and characterization of high-efficiency silicon wafer solar cells.

Prabir K. Basu received the B.Sc./M.Sc./M.S. and Ph.D. degrees in physics from several universities in India.

He is a Senior Research Scientist with the Solar Energy Research Institute of Singapore, National University of Singapore, Singapore. His research focuses on low-cost industrial high-efficiency silicon wafer solar cells.

Armin G. Aberle received the Physicist and Ph.D. degrees in physics from the University of Freiburg, Freiburg, Germany, in 1988 and 1992, respectively, and the Dr. rer. nat. habil. degree in physics from the University of Hannover, Hannover, Germany, in 1999.

He is the Chief Executive Officer with the Solar Energy Research Institute of Singapore, Singapore. He has published extensively ($>$300 papers), and his work has a high impact ($>$4000 citations). He is an Editor of several scientific journals. In the 1990s, he established the Silicon Photovoltaics (PV) Department at the Institute for Solar Energy Research Hamelin, Hamelin, Germany. He then worked for 10 years in Australia as a Professor of PV with the University of New South Wales, Sydney.